

# Magnetic properties and geochemistry of loess/paleosol sequences at Nowdeh section northeastern of Iran

Feizi, Vahid <sup>\*1</sup>, Azizi , Ghasem <sup>2</sup>, Mollashahi, Maryam <sup>3</sup>, Alimohammadian, Habib <sup>4</sup>

1- Ph.D. Dep. of Geography, Climatology, Tehran University, [Vahid.feizi62@gmail.com](mailto:Vahid.feizi62@gmail.com)

2- Professor., Dep. of Geography, Climatology, Tehran University, [ghazizi@ut.ac.ir](mailto:ghazizi@ut.ac.ir)

3- Assistant Professor of Forestry in Arid regions, Faculty of Desert Study, Semnan University, Iran [maryam.mollashahi@semnan.ac.ir](mailto:maryam.mollashahi@semnan.ac.ir)

4- Assistance Prof, Environment Magnetic Laboratory, Dep. of Geology and Mineral Exploration [halimohammadian@gmail.com](mailto:halimohammadian@gmail.com)

\*-Corresponding Author: Feizi,Vahid. Email: [vahid.feizi62@gmail.com](mailto:vahid.feizi62@gmail.com) Tell: 00989127985286

## Abstract

The loess-paleosol sequences in the northeastern part of Iran serve as a high-resolution natural archive documenting climate and environmental changes. These sequences offer evidence of the interaction between the accumulation and erosion of aeolian and fluvial sediments during the Middle and Late Pleistocene periods. In this study, the Azadshar (Nowdeh Loess Section) site was chosen to reconstruct Late Quaternary climate shifts. The 24-meter thick Nowdeh loess/paleosol sequence was sampled for magnetic and geochemical analysis. The sampling involved 237 samples taken systematically at high resolution (10 cm intervals, selected samples, corresponding to peaks in magnetic susceptibility, underwent geochemical analysis to aid in the interpretation of paleoclimatic changes indicated by the magnetic signals). The magnetic susceptibility results of the loess/paleosol deposits revealed low values during cold and dry climate periods (loess) and high values during warm and humid climate periods (paleosol). The magnetic susceptibility at a depth of 22.1 meters (approximately 130 Ka) has significantly decreased, suggesting cold climate conditions at this time. The most substantial changes in magnetic susceptibility occur at depths between 18.6 to 21.3 meters (approximately 100 to 120 Ka). During this period, there are four phases of decrease (indicating cold and dry conditions) interspersed with three phases of increase (signifying warm and humid conditions) in magnetic susceptibility. The comparison of magnetic and geochemical data showed that variations in geochemical weathering ratios corresponded to changes in magnetic parameters. A high level of correlation was observed between the magnetic susceptibility intensity and ratios such as Rb/Sr, Mn/Ti, Zr/Ti, and Mn/Sr. The findings from this research indicate that the sedimentary section of Nowdeh has experienced six distinct climate periods over the last 160,000 years. Notably, three cold and dry

periods occurred between three warm and humid periods. Additionally, during these climate phases, short-term cold (stadial) and warm (interstadial) intervals were also observed.

Keyword: Loess/paleosols sequences, Climate, Magnetic parameters, Geochemical proxies, Northeastern of Iran.

## **Introduction**

Reconstruction of the Quaternary climate is important for the development of climate models that lead to a better understanding of past and present and prediction of future climate development. Loess–paleosol sequences are now recognized as one of the most complete terrestrial archives of glacial–interglacial climate change (Porter, 2001; Muhs and Bettis, 2003, Pierce et al, 2011, Guo et al, 2002) and have been used to reconstruct climate and geomorphological changes during the Quaternary (Karimi et al., 2011; Frechen et al., 2003; Prins et al., 2007).

Loess deposits occur in large areas of the northeast, east central, north and central parts of Iran which is part of the loess belt that covers the Middle East and extends further northward into Turkmenistan, Kazakhstan and Tajikistan (Okhravi and Amini, 2001). The extensive and thick loess deposits in northern Iran have been recently studied in detail establishing a more reliable chronological framework for the last interglacial/glacial cycle (Lateef, 1988; Pashae, 1996; Kehl et al., 2006; Frechen et al., 2009, Karimi et al, 2009, Karimi et al, 2013, Okhravi and Amini, 2001, Mehdipour et al, 2012).

Paleoclimate studies of loess deposits based on rock magnetism and combined analyses of rock magnetism and geochemistry around the world have attained appreciable advances in the past few decades (Bader et al, 2024; Jordanova and Jordanova, 2024; Heller and Liu, 1984; Forster et al., 1996; Ding et al., 2002; Guo et al., 2002; Chlachula, 2011; Bronger, 2003; Baumgart et al., 2013, Guanhua, et al, 2014). These studies comprise loess-paleosol records that cover loess plateaus in China, Germany, Poland, Tajikistan, Austria, Ukraine, and the Danube catchment (Hosek et al, 2015, Ahmad and Chandra, 2013, Chen, 2010; Jordanova et al., 2011; Buggle et al., 2009; Fitzsimmons et al., 2012; Fischer et al., 2012; Jary and Ciszek, 2013; Baumgart et al., 2013; Schatz et al., 2014; Gocke et al., 2014).

Despite its suitable geographical location there is only a limited number of studies of loess deposits from the North of Iran. In this work we explore the

71 potential of loess deposits in northern Iran for reconstructing late quaternary  
72 climate/environmental change.

### 74 **Study area**

75 The Nowdeh section is exposed at about 20 km southeast of Gonbad-e Kavus  
76 and east of Azadshahr city. The Nowdeh river dissects a more than 24 m thick  
77 sequence of yellowish brown (10 YR 5/4) loess covering northeast dipping  
78 weathered limestone.

79 The study area (37° 05' 50" N and 55° 12' 58" E) is part of the Alborz structure  
80 and this structure continues beneath the Caspian Sea. This zone includes regions  
81 north of the Alborz fault and south of the Caspian Sea. Toward the east, the  
82 Gorgan-Rasht zone is covered with thick layers of loess.

83 The Nowdeh section was selected for this work due to earlier soil studies by Kehl  
84 et al (2005) and Frichen et al (2009) combined with the existence of 12 dates for  
85 this section (Figure1).

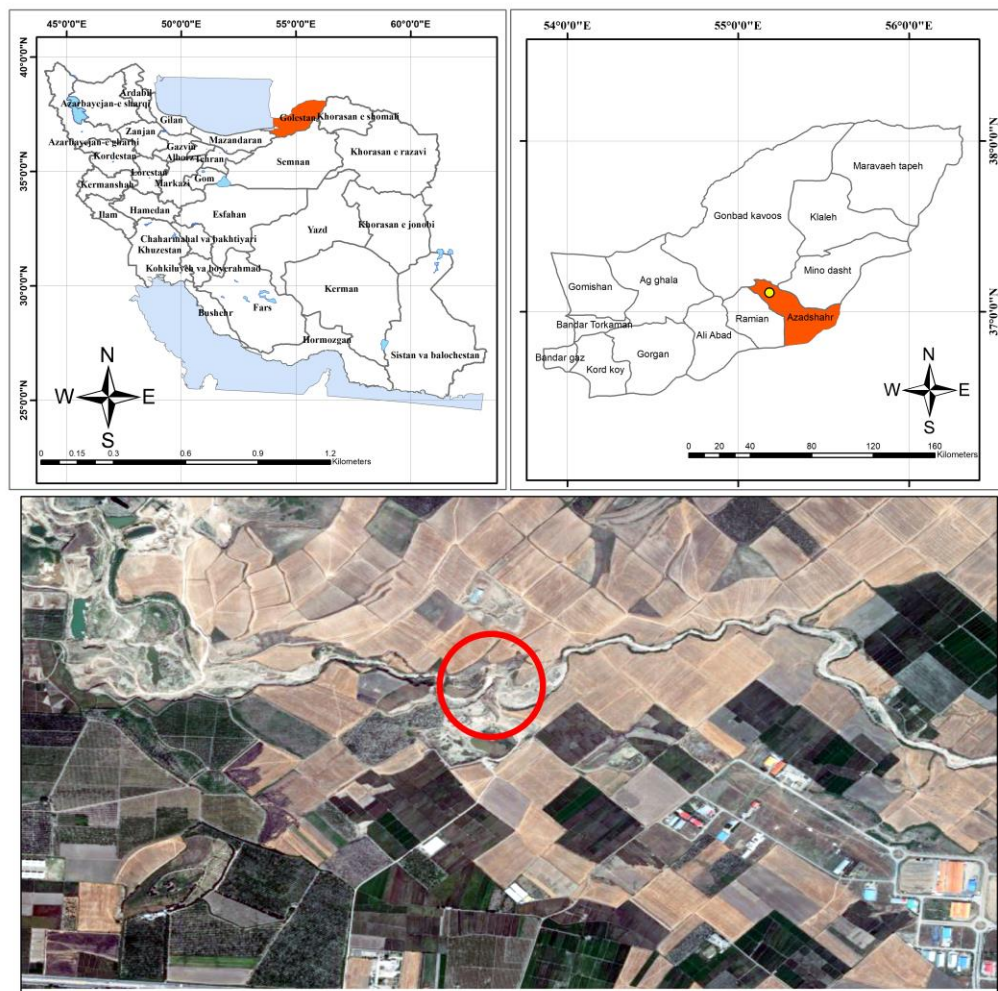


Figure 1: Map of Iran and the location of Nowdeh loess-paleosol sequence.



Figure 2: A view of the sedimentary section of the Nowdeh with its very clear layering.

## Methodology

The Nowdeh loess section is approximately 24 meters thick and was sampled at 10 cm intervals for magnetometry and geochemical analysis. The sampling location and method were determined following a detailed study of the area. Magnetic susceptibility measurements of all samples were conducted at the Environmental and Paleomagnetic Laboratory of the Geological Survey of Iran in Tehran. Magnetic susceptibility is indicative of the collective response of diamagnetic, paramagnetic, ferrimagnetic, and imperfect antiferromagnetic minerals present in the samples. Each sample was placed in a 11 cm<sup>3</sup> plastic cylinder for use in magnetic measurement devices. The measurement of magnetic susceptibility was performed using the AGICO Kappabridge model MFK1-A. To ensure the reproducibility of our results, we have meticulously documented all experimental procedures, including the setup, equipment used, and analytical methods. Our findings have been validated by testing multiple independent samples and conducting experiments repeatedly under controlled conditions.

The determination of the Saturation Isothermal Remanent Magnetization (SIRM) was carried out to assess the concentration of ferromagnetic and imperfect antiferromagnetic minerals in the samples. The calculation of the Hard Isothermal Remanence (HIRM) magnetization was performed to identify magnetically

significant components such as hematite in the samples using the following formula:

$$\text{HIRM} = 0.5(\text{SIRM} + \text{IRM} - 0.3T)$$

Where  $\text{IRM} - 0.3T$  is the remanence after application of a reversed field of 0.3 T after growth and measurement of SIRM. The HIRM reflects the contribution specifically of the imperfect antiferromagnetic minerals hematite and goethite (Bloemendal et al., 2008).

The  $S - 0.3T$  value, or S-ratio, is calculated as

$$S - 0.3T = 0.5[(-\text{IRM} - 0.3T / \text{SIRM}) + 1]$$

and it ranges from 0 and 100%. It reflects the ratio of ferrimagnetic to imperfect antiferromagnetic minerals (Bloemendal et al., 2008).

Based on the magnetic susceptibility results, 70 samples were selected for geochemical analyses (trace elements) to assist the paleoclimatic interpretation of the magnetic signals. Each sample was washed using a sieve with a mesh size of 400  $\mu\text{m}$  and then dried in an oven. Once dried, the samples were further sieved with a 325  $\mu\text{m}$  mesh sieve. The very fine sediments were collected, packed, and labeled as the tested material in special containers. A 0.2-gram portion of the powder from each sample was then placed in a 1 molar hydrochloric acid solution. After two hours, the samples were analyzed using an ICP device in the laboratory. The concentrations of the main elements were measured as a percentage, while the minor elements were quantified in milligrams per kilogram. To ensure the reproducibility of the results, we meticulously document all experimental steps, including the setup, equipment used, and analysis methods. The findings of this research have been validated through the use of multiple independent samples and by conducting experiments under controlled conditions.

As explained, the studied area was previously studied by Frichen et al. (2009) and Kehl et al (2005). Therefore, we chose this sedimentary section to investigate climate changes and used their dating data. The infrared stimulated luminescence (IRSL) technique is utilized for this dating. Forty-five samples were taken in light-tight tubes for the IRSL dating study. About 250 g of sediment was sampled. Polymineral fine-grained material (4–11 mm) was prepared for the measurements. The sediment material brought on disc was irradiated by a  $^{90}\text{Sr}/^{90}\text{Y}$  source in at least seven dose steps with five discs each and a radiation dose up to 750 Gy. All discs were stored at room temperature for at least 4 weeks after irradiation. The



irradiated samples were preheated for 1 min at 230 °C. De values were obtained by integrating the 1–10 s region of the IRSL decay curves. An exponential growth curve was fitted to the data and compared with the natural luminescence signal to estimate the De value. Alpha efficiency was estimated to  $0.08 \pm 0.02$  for all samples. Dose rates were calculated from potassium, uranium and thorium contents, as measured by gamma spectrometry (Germanium detector) in the laboratory, assuming radioactive equilibrium for the decay chains. The IRSL ages gradually increase with depth from  $20.5 \pm 2.0$  to  $103 \pm 10$  ka. The stratigraphically oldest sample was collected below the lowermost exposed strongly developed palaeosol (PC2) at a depth of 16.10m below surface. The about 10.50 m thick loess covering the uppermost strong paleosol (PC1) likely accumulated between about  $61.9 \pm 6.7$  and  $20 \pm 2.0$  ka (Frechen et al, 2009).

## **Results Magnetic properties**

In Figure 3, the relationship between susceptibility, NRM (Natural Remanent Magnetization), SIRM, HIRM, and S–0.3T in the Nowdeh section is illustrated. The variability in the magnetic susceptibility signal within the Nowdeh section indicates fluctuations in climate conditions and associated mechanisms during the Late Quaternary period. The values of magnetic susceptibility ( $\chi$ ) in the Nowdeh section range from 28.17 to 203.13 (in units of  $10^{-8} \text{ m}^3 \text{ kg}^{-1}$ ). The maximum  $\chi$  values (203.13) are found in the lower paleosol layer at 19.4 meters depth, while the minimum values are observed in the uppermost loess layer at 7.4 meters depth. The rock magnetic records exhibit a strong correlation with the lithology observed in the Nowdeh section. Generally, the paleosol layers exhibit higher magnetic signal intensities compared to the loess layers.

In figure 3 The paleosols exhibit higher magnetic susceptibility ( $\chi$ ) values compared to the loesses, with magnified magnetic enhancement observed in the Bw, Bt, and Btk horizons, while the underlying C (loess) horizon displays lower  $\chi$  values. This difference probably reflects precipitation of iron oxides in the Bw horizons, resulting in a higher concentration of pedogenetic magnetite in comparison to the C horizons (Jordanova et al., 2013; Hosek et al., 2015). As illustrated in Figure 3, the  $\chi$  values in the lower and middle sections of the Nowdeh profile, approximately 53-80 and 120-140 thousand years ago (Ka), (respectively at

depths of 9 to 15 and 18 to 23 meters), represent intermediate values between unweathered loesses and weathered paleosols.

The results indicate that the Natural Remanent Magnetization (NRM) is consistent with the variance in magnetic susceptibility, particularly notable at lower depths, with the highest recorded value of this parameter observed at 13.1 meters depth in the BW, BWK horizon (figure 3). Variations and discrepancies in magnetic susceptibility align closely with the SIRM values of the Loess sequence. As magnetic susceptibility decreases, SIRM also shows a corresponding decrease. In the interval between 20 to 50 thousand years ago (ka (Depth 2.1 to 8.4 meters), during which much of the upper Loess formation occurred, magnetic susceptibility shows minimal variation, a pattern mirrored in the SIRM diagram for this period. The elevated HIRM values in Figure 3 suggest an increase in the concentration and frequency of magnetic deterring minerals such as goethite, maghemite, or hematite.

In figure 3, the comparison between the lower values of saturation (S) (-0.3 T) (between 0.6 to 0.12 Am/m) and the higher values of Hard Isothermal Remanent Magnetization (HIRM) (between 2 to 5 Am/m) indicates that the proportion of minerals with lower saturation, such as magnetite, is significantly lower than the proportion of minerals with higher saturation in paleosols. This pattern contrasts with the composition of loess deposits. As illustrated in Figure 3, This can be clearly seen in loess sediments, for example, at a depth of 1 to 9 meters, representing the time interval between 18 and 52 ka.



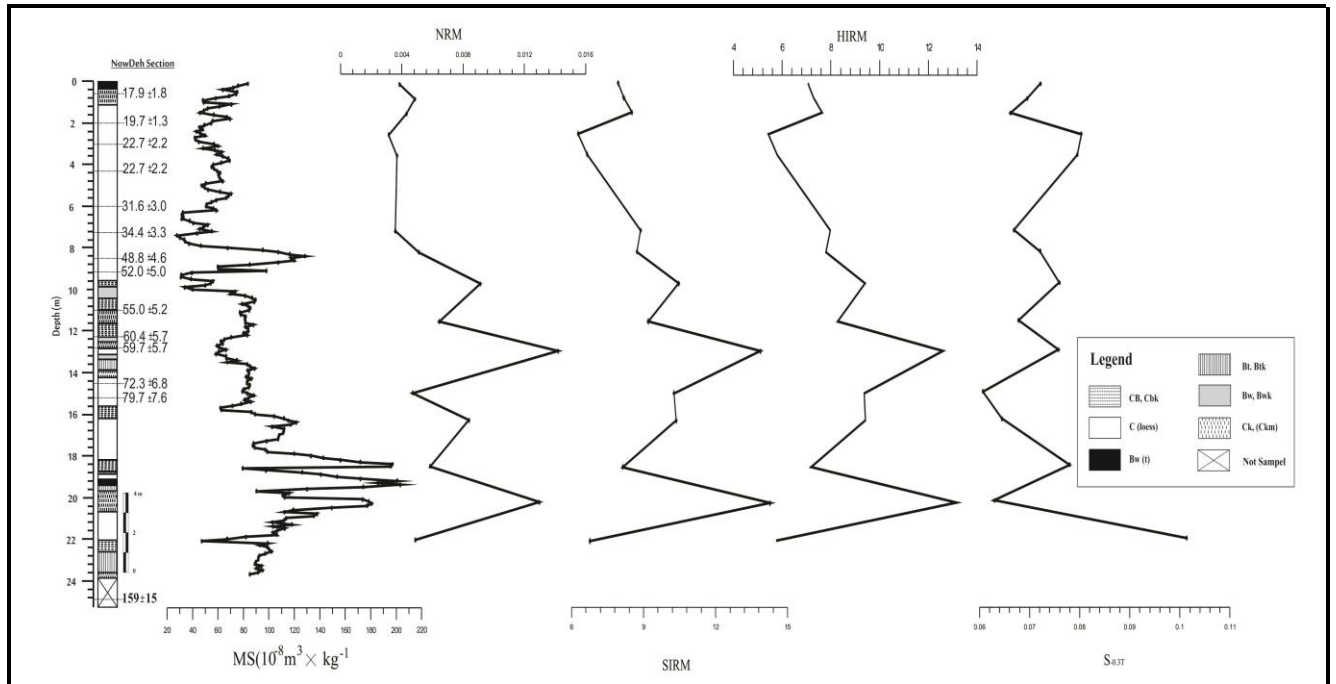


Figure 3: Basic magnetic parameters for Nowdeh section. (From left to right: a simplified lithological column, magnetic susceptibility (MS), natural remanent magnetization (NRM), isothermal remanent magnetization (SIRM), and S-ratio (S-0.3T) are plotted against depth (meters). The lithological column indicates the following sedimentary units: CB/Cbk (calcareous brown soil/calcareous brown soil with krotovina), C (loess), Bw(t) (brown soil with clay illuviation), Bt/Btk (brown soil with clay illuviation/calcareous brown soil with clay illuviation), Bw/Bwk (brown soil/calcareous brown soil), and Ck/(Ckm) (calcareous horizon/calcareous horizon with soft masses of calcium carbonate).

## Element stratigraphy

Figure 4 illustrates the correlation between the concentration of selected elements (Sr, Rb, Zr, Ti, and Mn) and magnetite susceptibility in the Nowdeh section. The figure indicates significant variations in the concentration of these elements with noticeable differences between them. Sr and Rb exhibit similar trends along the Nowdeh section. At a depth of 2.9 meters, there is a notable increase in the concentration of these two elements, corresponding to an age of 22 ka. Higher in the section, the concentration of Sr and Rb decreases.

In figure 4, at a depth of 18 meters, the Nowdeh sedimentary section recorded the highest concentrations of elements such as (Sr, Rb, Zr, Ti and Mn). Conversely, the lowest concentrations of these elements were observed at a depth of 8.5 meters, which dates back approximately 48 Ka.

In figure 4, Ti, Zr, and Mn exhibit approximately similar trends in the diagram. These elements show little variation in concentration at the beginning of the section. The changes in element concentrations from the end of the sedimentary section down to a depth of 16.7 meters (approximately 90 ka) display a zigzag pattern. Between the depths of 16.7 and 9.3 meters, the fluctuations in element concentrations are minimal. At a depth of 9.3 meters, corresponding to roughly to 52 ka, the research indicates the lowest concentrations of the elements measured. However, from this point onward, the concentration of elements begins to rise, peaking at a depth of 8.5 meters, which dates back to about 48 ka. This increase suggests a period of hot and humid conditions during that time.

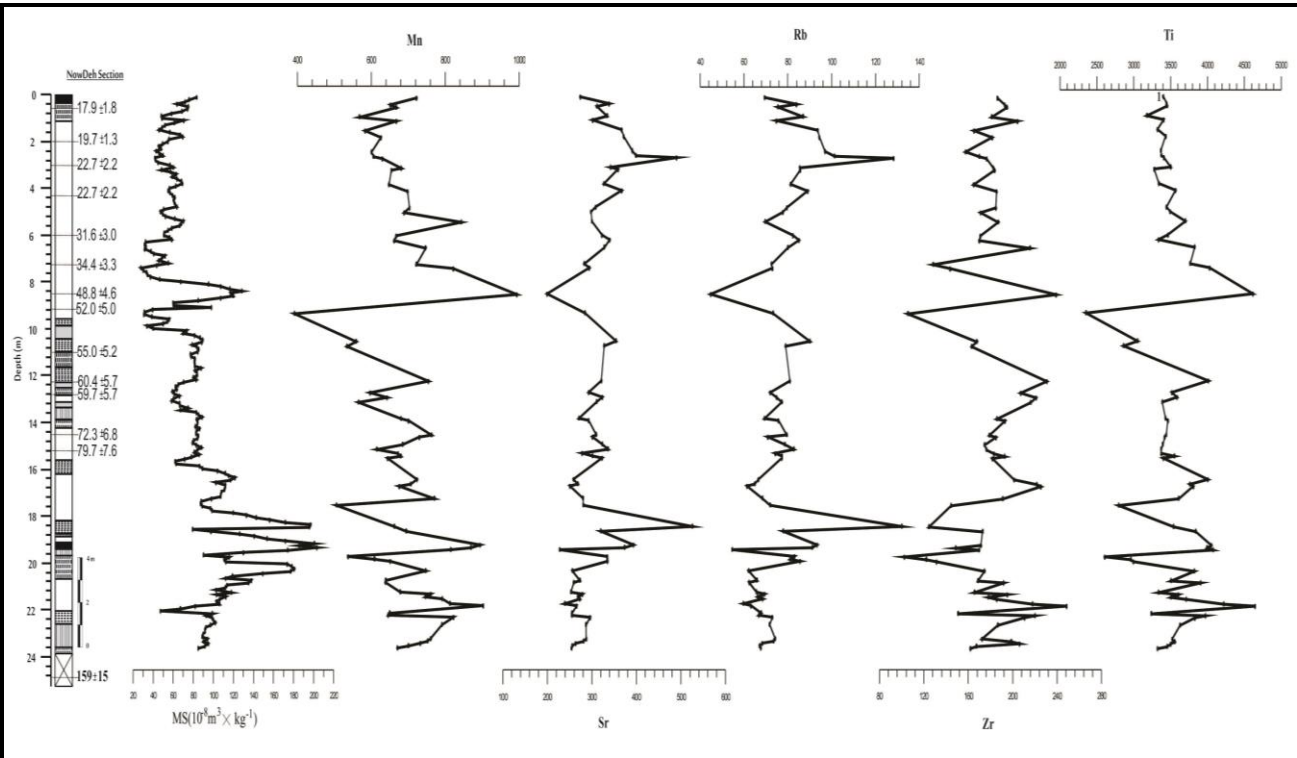


Figure 4: shows depth series of selected element concentrations for Nowdeh section.

### Trace element ratio

The variation of the Si/Ti ratio in figure 5 generally follows the magnetic susceptibility pattern (figure 5), except for the lower part of the section (23-24 meters). The ratios of Mn/Sr, Zr/Ti, and Mn/Ti in figure 5 show almost no long-term change, except for at a depth of 8.5 meters, corresponding to an age of 48.8 ka. These changes suggest hot and humid climatic conditions, which can be correlated with the high level of magnetic susceptibility. The Rb/Sr ratio exhibits

an opposite pattern to the magnetic susceptibility, especially at the depths of 8.5, 16, 19, and 22 meters. The Ba/Rb ratio generally follows the magnetic susceptibility pattern, except at depths of 13, 15, 19, and 22.8 meters where they vary oppositely.

The variation in the Si/Ti ratio does not exhibit a consistent relationship to the sequence of loess/palaeosol layers, as defined by the magnetic susceptibility in the Nowdeh section. On the other hand, the Mn/Ti ratios tend to show elevated values in the palaeosols, likely due to the concentration of Mn oxide in the finer sediment fraction (Bloemendal et al., 2008). This suggests that the presence of Mn oxide plays a significant role in influencing the Mn/Ti ratio in the sediments, particularly in the palaeosol layers.

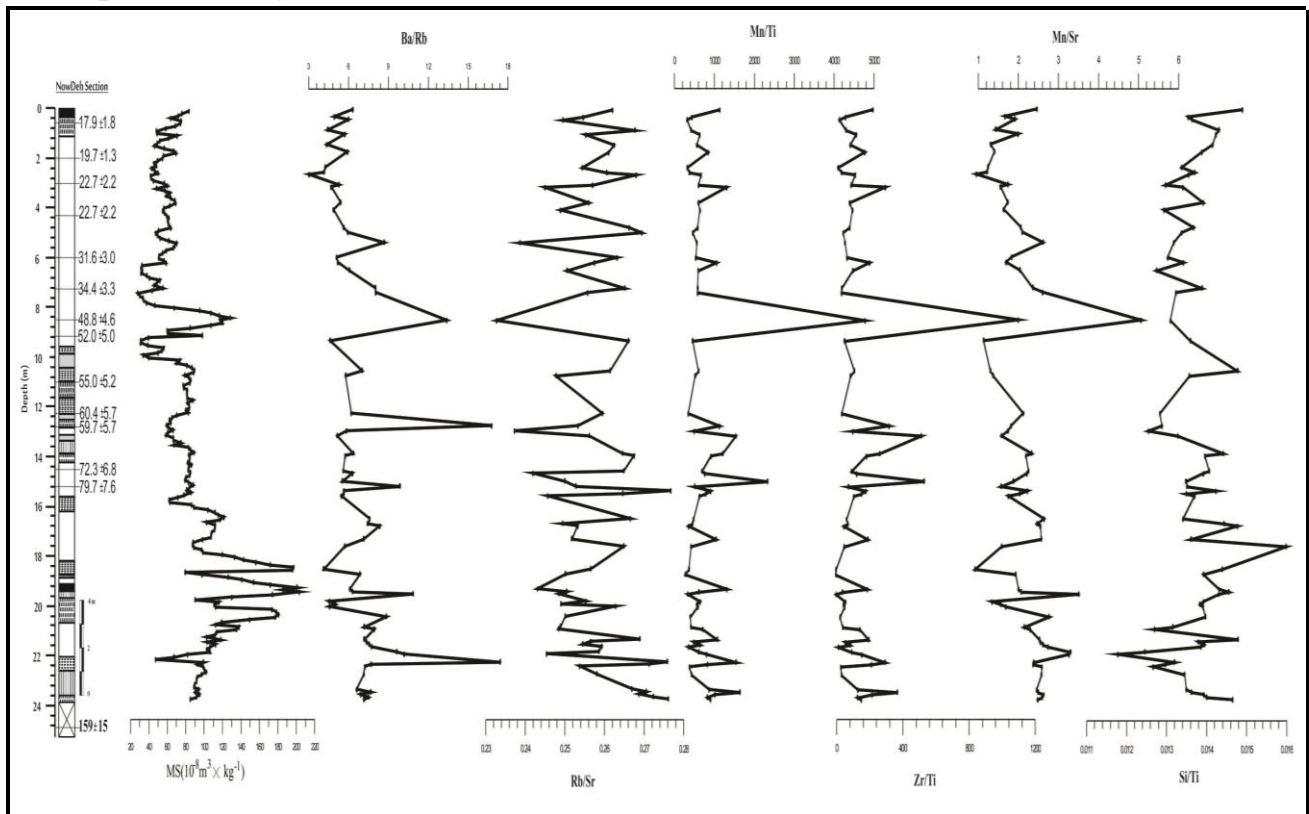


Figure 5: show selected element ratios in Nowdeh section

## Discussion

Over the entire 159 Ka sequence at the Nowdeh site, there appears to be a reasonable first-order co-variation between the magnetic and geochemical indicators of weathering and soil formation, particularly with magnetic parameters reflecting variations in ferrimagnetic content and Sr-based ratios. However, upon

closer detailed examination based on individual loess and palaeosol layers, an inconsistent relationship is observed between the amplitudes of individual peaks and troughs of magnetic and geochemical parameters (Fig 4 and 5). This suggests that while there is an overall correlation between these indicators at a broader scale, at a finer resolution within specific layers, the relationship becomes more complex and inconsistent. Additional factors or processes may be influencing the variations in magnetic and geochemical parameters within the individual stratigraphic units. This issue can be seen clearly in Figures 4 and 5. As noted by Hosek et al (2015) and Makeey et al (2024), there is a significant relationship between magnetic receptivity, chemical elements, and climatic conditions. Our study reinforces this finding, as indicated by the results obtained. Recent studies have highlighted a significant relationship between climate change and the magnetic properties of sediments, indicating that alterations in sediment composition and depositional environments can reflect past climate conditions. For instance, Huang et al. (2022) demonstrated that variations in magnetic susceptibility in loess deposits are closely linked to fluctuations in moisture levels and temperature, underscoring the sensitivity of magnetic minerals to climatic changes. These findings suggest that analyzing the magnetic properties of sediments can provide valuable insights into historical climate dynamics and contribute to our understanding of how magnetic signatures may evolve in response to ongoing climate change. To investigate the relationship between climate change and the magnetic properties of sediments, we conducted magnetic susceptibility measurements on loess sediments from the Nowdeh section. The results of the magnetic susceptibility analysis demonstrated clear patterns that correlate with historical climatic fluctuations (fig 3). The observed distinct sequences in magnetic susceptibility reveal insights into past environmental conditions, with lower values indicating cold and dry periods typical of loess deposition, while higher values correspond to warmer and more humid phases associated with paleosol development. These correlations between magnetic susceptibility and alternating loess-paleosol sequences provide a compelling illustration of how sediment magnetic properties reflect climatic changes over time in the Nowdeh region. The implications of these findings are significant, as they suggest that magnetic susceptibility can serve as a reliable proxy for reconstructing paleoclimatic conditions. By establishing this relationship, we enhance our understanding of how the sedimentary environment responded to climate shifts during the Pleistocene. Furthermore, these patterns of magnetic susceptibility not

only inform us about specific climatic conditions but also help elucidate the feedback mechanisms between climate and weathering processes in the region. In essence, our analysis underscores the potential of magnetic susceptibility as a key indicator of past climate change, linking geological records with broader climatic events. This enhanced understanding is crucial for interpreting how similar climatic fluctuations may affect sediment dynamics in other regions with comparable loess deposits.

According to Song et al. (2008), sediment loess is typically formed under cold and dry climate conditions, leading to lower magnetic susceptibility values due to minimal weathering processes. This observation aligns with the findings in the Nowdeh section, where our data indicate that the loess layers are characterized by significantly lower magnetic susceptibility than the overlying paleosols (fig 3). In the paleosols of the Nowdeh section, formed through extensive pedogenic processes, we observe elevated magnetic susceptibility attributed to increased levels of oxidation and enhanced concentrations of key elements such as iron and aluminum oxides (fig3). Our magnetic susceptibility data corroborate the assertion by Song et al. (2008) that paleosols generally exhibit higher magnetic susceptibility compared to adjacent loess layers. Specifically, our measurements indicate a distinct rise in magnetic susceptibility values within these paleosols, further supporting the notion that the formation of strong magnetic minerals, such as iron oxides ( $\text{Fe}_3\text{O}_4$ ,  $\gamma\text{-Fe}_2\text{O}_3$ , and  $\text{Fe}_2\text{O}_3$ ), occurs through pedogenesis. Moreover, the composition of magnetic minerals in our loess samples is influenced by the grain composition from the aeolian sources of sedimentation. This distinction is crucial, as our data illustrate a clear contrast in magnetic mineral content between the well-developed paleosols and the less altered loess layers. In our analysis, we found that the paleosols not only have higher magnetic susceptibility but also exhibit a more diverse range of magnetic mineral types, indicating a more complex pedogenic history. This relationship highlights the importance of understanding the processes of magnetic mineral formation and alteration in determining the magnetic susceptibility profiles of sediment sequences. Our own findings reinforce the established understanding from previous studies, such as those by Song et al. (2008), while providing new insights into the specific conditions and processes at play in the Nowdeh section.

In Fig. 3, the brown layer sequences of dark and light paleosols within the loess deposits illustrate distinct weathering processes that reflect the climatic patterns

observed during glacial and interglacial periods of the middle and late Pleistocene. The higher magnetic susceptibility of the paleosols compared to the surrounding loess layers indicates a significant degree of pedogenesis and oxidation, consistent with findings by Maher (2011) and Spassov (2002). This difference is particularly pronounced at lower depths, suggesting that these layers experienced greater weathering variability during those periods. At a depth of 21 meters (approximately 110 ka), the notable decrease in magnetic susceptibility suggests a transition to colder and drier conditions, which aligns with the known climatic shifts of that era. This finding is crucial because it highlights how magnetic susceptibility can serve as a proxy for past climatic conditions, providing insights into the environmental changes that influenced soil development (Thompson & Oldfield, 2021; Liu et al., 2022). The magnetic susceptibility chart for the Nowdeh section reveals around eight distinct periods of increasing magnetic susceptibility, indicative of elevated temperatures and humidity, consistent with findings from other regions that link magnetic properties to climatic variations (Dearing et al., 2023; Heller & Liu, 2020). This pattern suggests a correlation between magnetic susceptibility and climatic conditions, where periods of increased susceptibility correspond to warmer, more humid phases conducive to soil formation.

In accordance with the standard global loess characteristics, paleosols consistently exhibit higher magnetic susceptibility values compared to adjacent loess layers due to pedogenesis and oxidation processes, as highlighted by Maher (2011) and Spassov (2002). The NRM results suggest a decrease during loess formation and an increase during paleosol formation (figure 3). This pattern suggests a relationship between NRM and magnetic susceptibility figure 3 (Bloemendal et al., 2008). A decrease in NRM indicates dry and cold climate conditions in figure 3 (at the depth of 7.2 meters, which is approximately equal to 34 Ka), consistent with the deposition of loess layers, while an increase in NRM represents warmer and more humid climate conditions, corresponding to paleosol formation. The results presented in the previous section illuminate the significant relationship between NRM (Natural Remanent Magnetization) and magnetic susceptibility, contributing to our understanding of past climatic conditions. The observed decrease in NRM at a depth of 7.2 meters (approximately 34 ka) is indicative of drier and colder climate conditions, consistent with the processes associated with loess deposition. This finding reinforces the notion that periods of extensive loess accumulation correspond with colder climatic phases, as seen in other studies of similar

stratigraphic sequences. Conversely, the increase in NRM at depths of 18.6 to 21.3 meters marks a shift toward warmer and more humid conditions, which correlates with paleosol formation. This transitional phase highlights the dynamic interplay between climate and soil development, suggesting that optimum conditions for soil formation fostered the development of paleosols during this time. The highest magnetic susceptibility values in this layer, documented in Fig. 3, further corroborate the enhancing environmental conditions during this interval. The peak alignment of NRM and magnetic susceptibility at a depth of 19.4 meters, approximately 120 ka, is particularly noteworthy. This correlation may signify a period of climatic stability that allowed for the establishment of rich soil profiles, crucial for understanding the ecological dynamics at play during the late Pleistocene. Such findings align with previous research by Bloemendal et al. (2008), which also emphasized the relevance of magnetic properties in interpreting paleoclimatic conditions.

The probable justifications for the low alteration in magnetic susceptibility and isothermal remnant magnetization between 20 to 50 Ka (Figure 3) can be attributed to two main factors:

- 1- Decreased Pedogenesis due to cold and dry periods.
- 2- Reduction in the influx of magnetic particles into loess layers.

During the last 20 ka, there seems to be a correlation between magnetic susceptibility variations in the surface soil layer and climatic conditions. This period coincides with the transition from cold climate to the current warm and humid climate in the northern region of Iran (Frichen et al, 2009). As a result, the soil's magnetic properties, specifically SIRM, have likely increased during this time frame. However, since the SIRM samples were only collected at magnetic susceptibility peak points, they may not capture the full extent of variations. Comparing these findings with the research by Antoine et al. (2013) on loess/paleosol sediments in Central Europe reveals a close relationship, particularly around 32 ka. The close relationship observed in our findings and those of Antoine et al. (2013) around 32 ka suggests a synchronous response of the magnetic susceptibility of sediments to environmental changes during this period. This synchrony reinforces the idea that widespread climatic or geological factors were influencing sediment formation across regions. Also, Antoine et al. (2013) provided critical insights into the paleoenvironmental conditions in Central Europe during the Late Pleistocene.



Geochemical charts can serve as useful indicators of Climate patterns, as they can highlight different levels of weathering severity. In the study of loess deposits, certain chemical ratios can be utilized to reconstruct variations in paleoclimate (Ding et al., 2001). The Zr/Ti, Mn/Ti, Rb/Sr, and Mn/Sr records from the Nowdeh section exhibit a clear pattern of higher values prevailing in the palaeosols, and their high degree of similarity is noteworthy. Rb/Sr has been suggested by several researchers as an indicator of pedogenic intensity in loess, based on the differential weathering of the major host minerals, specifically K-feldspar for Rb and carbonates for Sr (Hosek et al, 2015, makeey et al, 2024). In the case of Mn/Sr, the higher values observed in the palaeosols are likely a result of the combined effects of grain size on Mn concentration, as well as the loss of Sr through solution processes. This indicates that these ratios can serve as important indicators of pedogenic processes and weathering dynamics in the sedimentary record of the Nowdeh section. Rubidium is derived from K-feldspar, while strontium comes from carbonate minerals. As soils weather, an increase in Rb/Sr often indicates selective retention of Rb while Sr is leached away, reflecting greater weathering intensity (Bai et al., 2022). Climate-driven changes, such as increased precipitation, can enhance Sr leaching, leading to higher Rb/Sr ratios in wetter conditions. This relationship highlights how climate influences elemental cycling in soils (Zhang et al., 2021).

The magnetic susceptibility record shows high values at a depth of 19.4 meters(fig3), indicating hot and humid climate conditions prevailing around 120 ka. Variations in the concentrations of manganese (Mn), zirconium (Zr), and titanium (Ti) in the soil reflect a clear stratigraphic pattern (figure 4), with higher values seen in paleosols and lower values in the loess layers (Bloemendal et al., 2008). This pattern is influenced, in part, by carbonate dilution/concentration effects, as a significant portion of the variability in these elements disappears when expressed on a carbonate-corrected basis. In a study by Chen et al. (1999), a comparison was made between the Rb/Sr ratios and magnetic susceptibility values in the uppermost (last glacial/interglacial) sections of the Luochuan and Huanxian regions. The researchers noted a remarkable correspondence between the amplitudes of variation in magnetic susceptibility and Rb/Sr ratios. This finding suggests a close relationship between magnetic susceptibility variations and the Rb/Sr ratios in these regions during the last glacial and interglacial periods.

In the Nowdeh section, the amount of rubidium (Rb) in paleosols was lower compared to its concentration in loess layers (Figure 5). This discrepancy can be attributed to the higher solubility of Rb in warm and humid climates, typical of interglacial periods. Gallet et al. (1996) observed significant depletion of Rb in the paleosols, supporting this interpretation. Recent research by Zhu et al. (2021) demonstrated that climate change alters the biogeochemical cycling of nutrients, including Rb, leading to increased leaching in saturated soils during periods of heavy rainfall. Additionally, studies by Arias-Ortiz et al. (2020) highlighted that changing climate conditions contribute to shifts in soil chemistry and nutrient availability, affecting soil formation and stability. Their findings underline the complex interactions between climate variations and elemental behavior in soil profiles. Furthermore, a comprehensive review by Jiang et al. (2020) emphasized the impacts of climate change on soil properties, particularly focusing on leaching processes and the resultant changes in nutrient concentration due to increased precipitation and temperature.

Our results indicate that the Mn/Ti, Zr/Ti, and Mn/Sr ratios tend to exhibit higher values in the paleosols (fig4). According to Ding et al. (2001), elevated Mn/Ti values in paleosols may result from the concentration of iron (Fe) and manganese (Mn) oxides in the finer sediment fractions. They also noted that the Rb/Sr and Mn/Sr ratios show a clear pattern of elevation in the paleosols, which aligns with the findings of our study (figure 5). The Rb/Sr ratio has been proposed by various researchers as an indicator of pedogenic intensity in loess deposits, based on the differential weathering of major host minerals such as K-feldspar for Rb and carbonates for Sr. The higher Mn/Sr values in paleosols may be attributed to grain-size effects on Mn concentrations and the solubilization loss of Sr.

Chen et al. (1999) compared Rb/Sr and magnetic susceptibility in the uppermost parts of the Luochuan and Huanxian sections, revealing a significant correspondence between the variations in magnetic susceptibility and Rb/Sr ratios. This suggests a link between weathering intensity and magnetic properties in these sediments. In the context of the Nowdeh sedimentary section, the magnetic parameters were compared with those from other studies conducted in various regions of the world, further contributing to our understanding of paleoclimatic variations and weathering processes in loess deposits.

In figure 6 the comparison of magnetic receptivity results from the Nowdeh sedimentary section with the palynological data from sedimentary cores of Urmia

Lake (Djamali et al., 2008) and the  $^{18}\delta$  analysis from Arabian Sea sedimentary cores (Tzedakis, 1994) has provided valuable insights into past climate conditions (Figure 6). In the analysis, an increase in the AP/NAP index (Arboreal Pollen grains (AP) to that of the Non-Arboreal Pollen grains (NAP)) in the lakes corresponded with the presence of ancient soil layers in the seedling sedimentary section.

This increase signifies warmer temperatures and higher humidity levels, conducive to the growth of trees and shrubs (Harrison et al., 2020; Zhang et al., 2021). Conversely, a decrease in the AP/NAP index indicates a decline in temperature and humidity, leading to the disappearance of trees and shrubs and changes in surface vegetation cover (Chen et al., 2022). This correlation suggests that the climate conditions and their fluctuations in western Iran align with the sedimentary deposition at Nowdeh, consistent with findings from similar studies in the region (Fuchs et al., 2013; Hosek et al., 2015).

Moreover, in figure 6 the  $^{18}\delta$  analysis of the Arabian Sea exhibited a strong agreement with magnetic receptivity data. A decrease in the  $^{18}\delta$  indexes points to warmer climate conditions, while an increase indicates colder conditions (Djamali et al, 2008). The relationship between magnetic susceptibility and  $^{18}\delta$  levels in the Arabian Sea sediments, as shown in Figure 6, Verifies that an increase in magnetic susceptibility corresponds with a decrease in  $^{18}\delta$  levels, indicating warmer climate conditions. This alignment further supports the connection between the recorded palynology data of Lake Urmia,  $^{18}\delta$  data from the Arabian Sea, and the sequence of ancient loess-soil sediments in the Nowdeh sedimentary section.

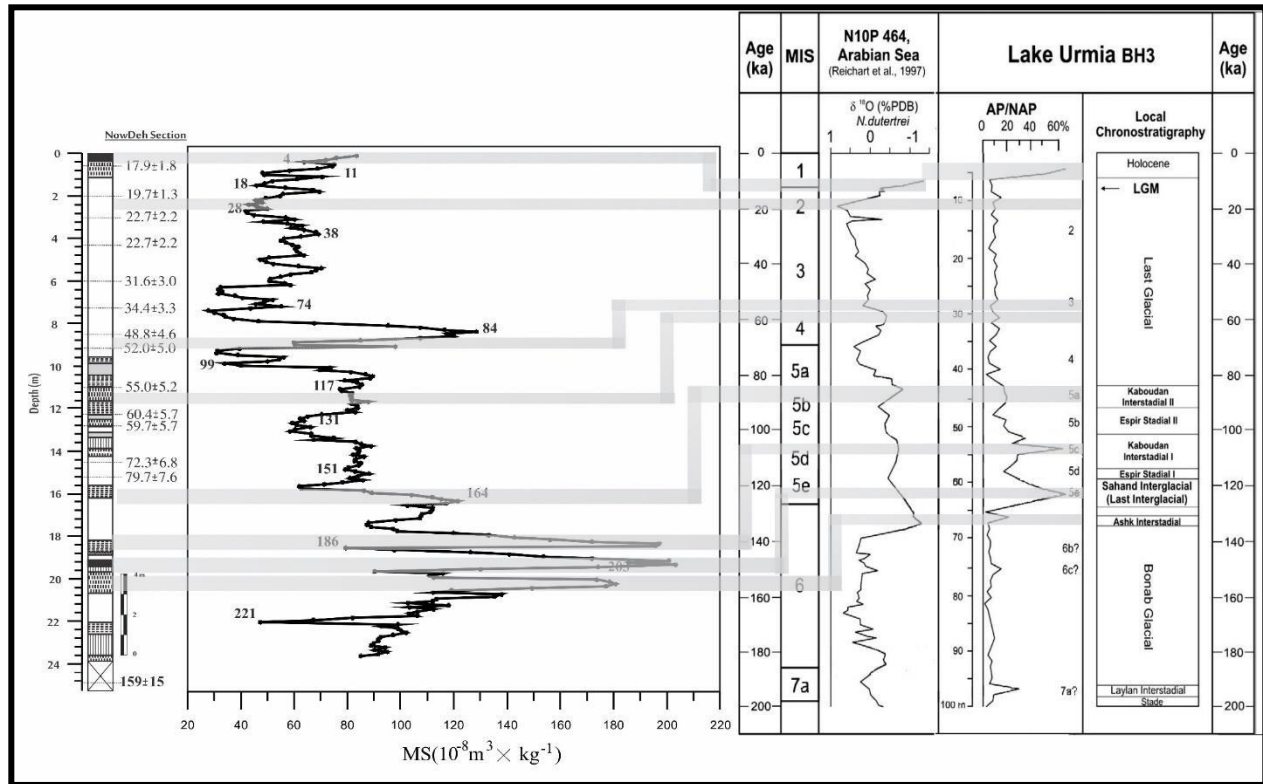


Figure 6: Correlation between recorded palynological data of Lake Urmia (Djamali et al, 2008) and  $^{18}\delta$  of Arabian Sea sediments (Tzedakis, 1994) with the Loess-Paleosol sediment sequence of Nowdeh sedimentary section.

The results of our current research demonstrate a significant correlation with the findings of Fuchs et al. (2013) and Hosek et al. (2015), which examined ancient loess and paleosol deposits in Central Europe, indicating that similar magnetic properties can be observed across different regions in response to climate change. Figure 8 depicts consistent patterns in the magnetic receptivity parameter at 45, 73, 90, 104, and 108 ka across the study sections. Around 45 and 73 ka, there is a clear increasing trend in magnetic receptivity observed in all analyzed layers, indicating a shift towards warmer and more humid climate conditions compared to earlier periods. This increase in magnetic susceptibility can be attributed to the higher presence of iron oxides in the soil resulting from increased chemical weathering. Conversely, during the periods of 90, 104, and 108 ka, a decrease in magnetic susceptibility is evident across all regions, signifying colder and drier climatic conditions during these time intervals. This issue can also be seen in the amount of  $\text{Fe}_2\text{O}_3$  in Nowdeh sediments (Figure 7). While the older sediments also show a significant association with climate variations in Central Europe and the Nowdeh



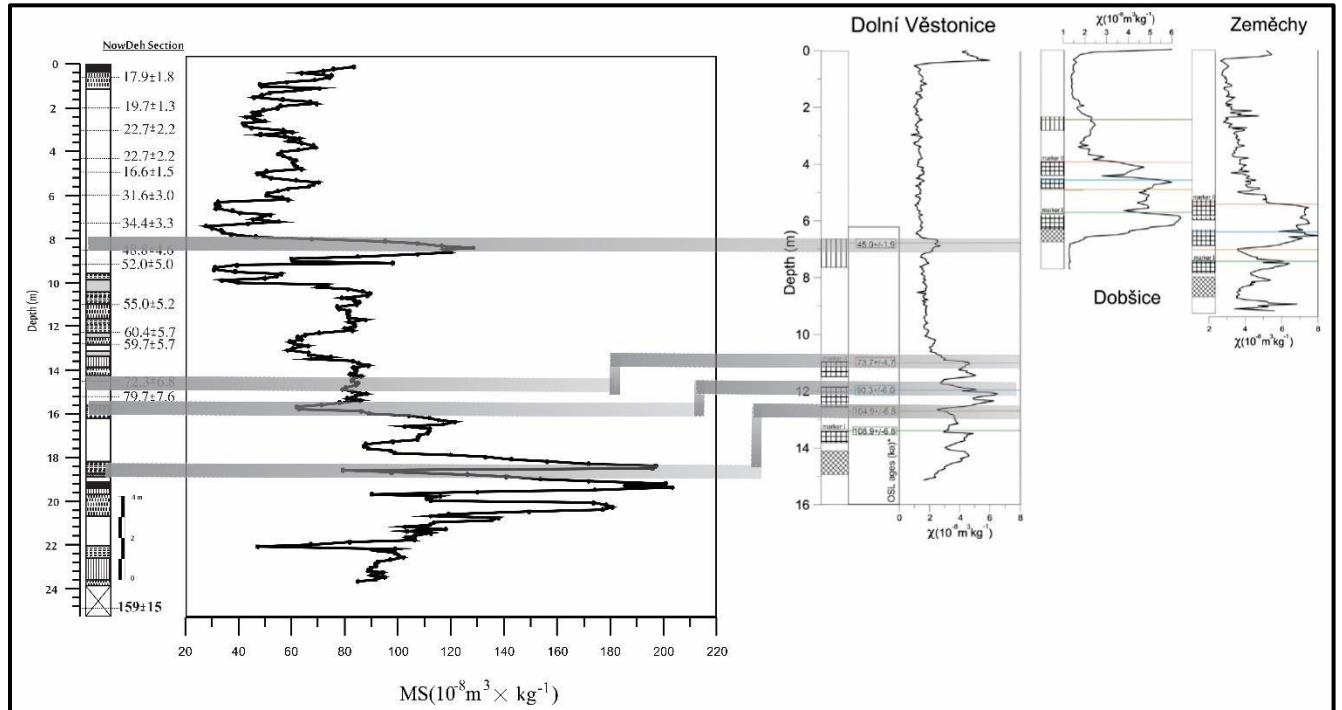


Figure 8: Comparison of changes in magnetic receptivity of Dolní Věstonice sedimentary section, Fuchs et al, 2013, Dobšice and Zeměchy section, Hošek et al, 2015, with Nowdeh sedimentary section

The comparison of magnetic receptivity trends as recorded in sedimentary sections of Beiyuan, Heimugou, Biampo, and the  $^{18}\delta$  records by Imbrie et al. (1984) in Figure 9 reveals a high agreement with the Nowdeh sedimentary section. This alignment indicates similar climate conditions across different locations in the Northern Hemisphere.

The consistency in magnetic receptivity trends among these various sites suggests a commonality in the climatic conditions experienced during the corresponding time periods. This synchronization in magnetic susceptibility patterns further supports the notion that these regions were subjected to comparable environmental changes and fluctuations in the past.

Additionally, the correlation observed between the magnetic receptivity data and the  $^{18}\delta$  records underscore the close relationship between climatic factors and sedimentary deposition patterns across these sites (Figure 9). By examining these geological proxies, researchers can gain valuable insights into the past climate dynamics and variations that have affected the Northern Hemisphere over time.

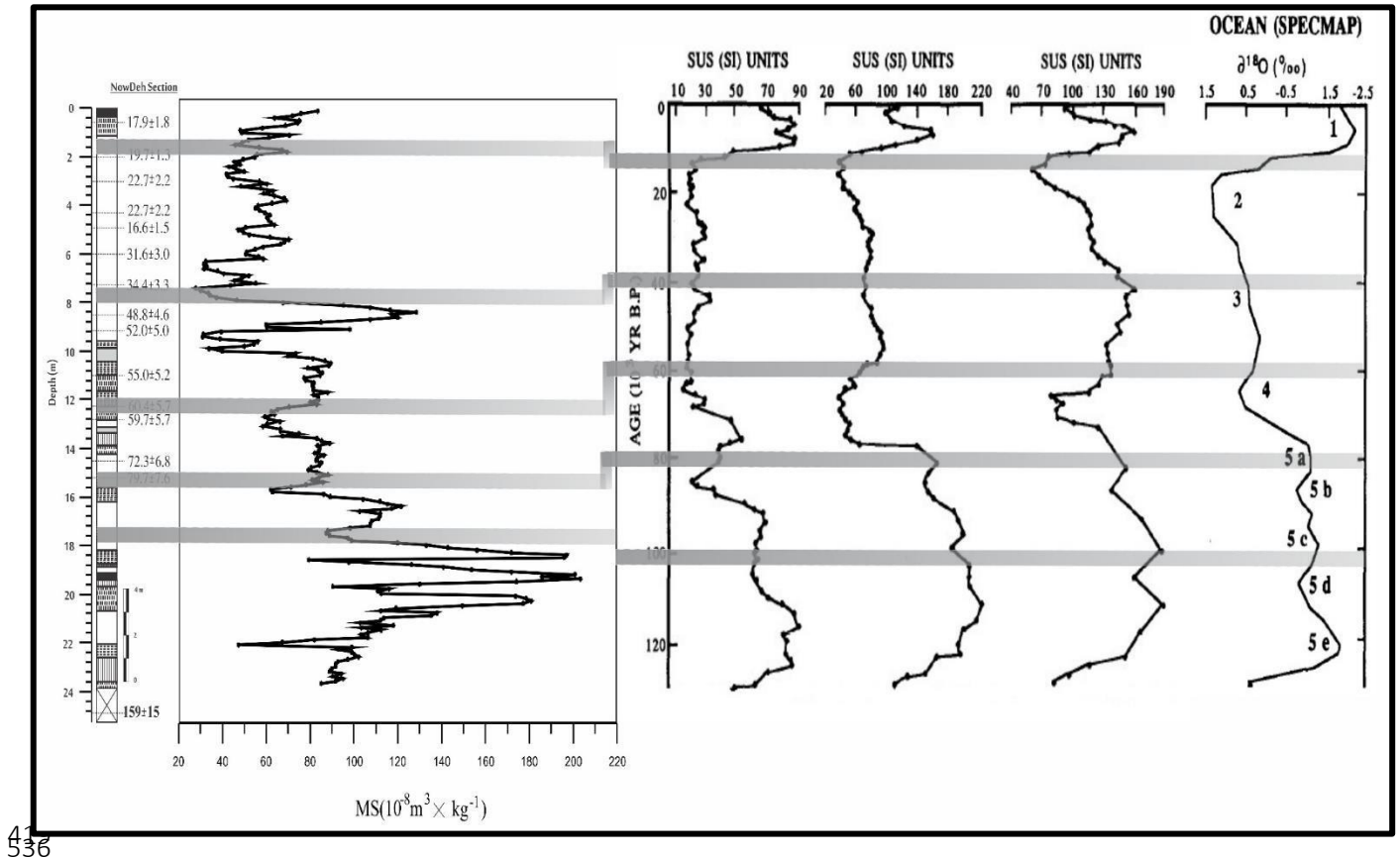


Figure 9: Comparison of magnetic receptivity changes of Bei yuan, Heimugou, Biampo, An et al, 1991, records of  $^{18}\delta$  Imbrie et al, 1984 with Nowdeh sedimentary section

The findings of Mehdipour et al. in 2012 in the realm of fine loess exhibit a close resemblance to the results presented in our research, as illustrated in Figure 9. In their study, they employed both magnetic and geochemical approaches to assess different climatic periods, and the outcomes align significantly with the findings of our research. The comparison in Figure 10 reveals a strong consistency in the magnetic receptivity trends between the Nowdeh section and the Neka sedimentary section analyzed by Mehdipour et al (2012). Between 48 and 20 thousand years ago, notable similarities are observed in the fluctuations of magnetic receptivity in both sedimentary sections. Whenever there is an increase in magnetic receptivity, it indicates a warm and humid period with the formation of ancient soil layers. This shared pattern implies a synchrony in climatic conditions between the two regions during this time frame, showcasing the utility of magnetic susceptibility as a proxy for understanding past environmental changes and soil development processes.



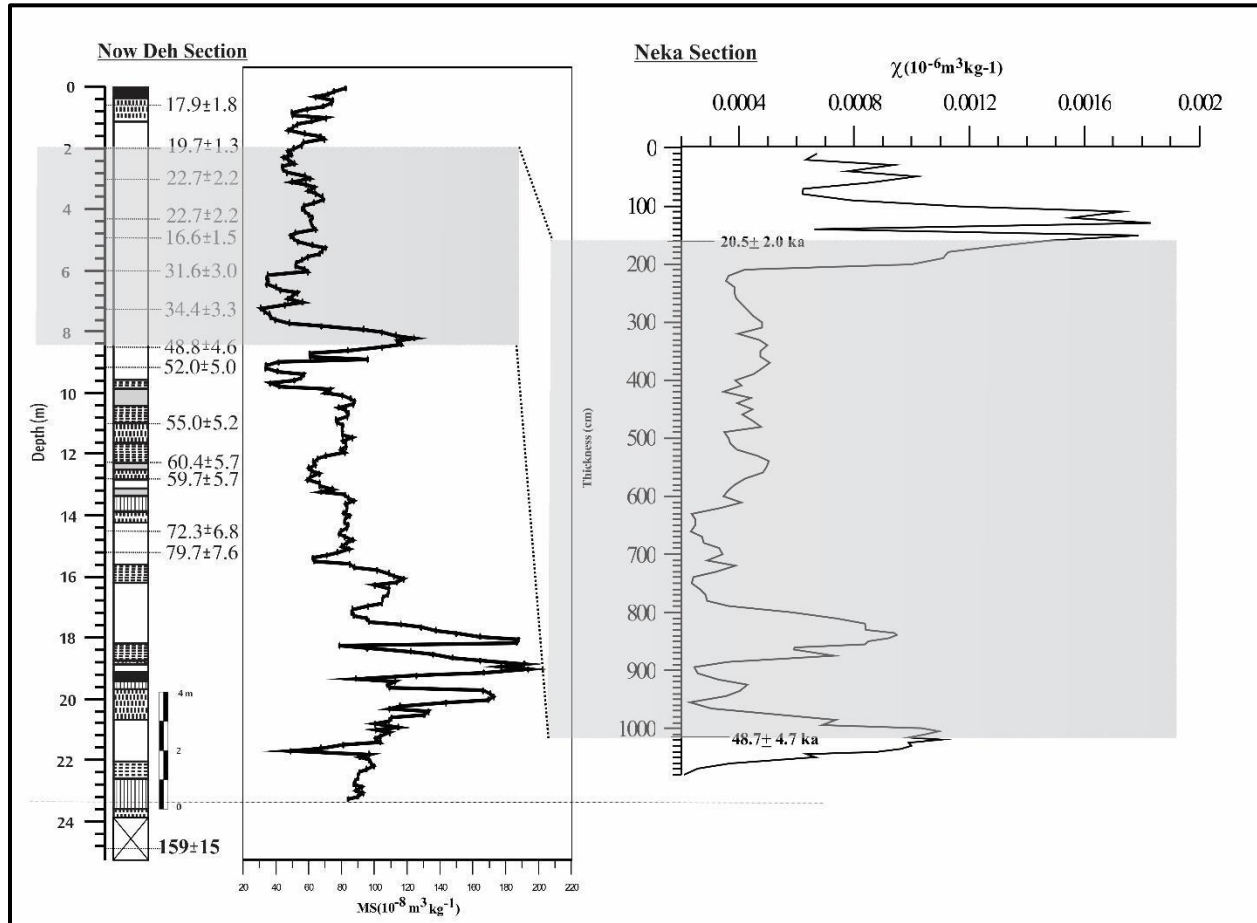


Figure 10: Comparison of magnetic receptivity diagram of Nowdeh sedimentary section with Neka sedimentary section (Mehdipour et al., 2012)

The results of this research exhibit a strong consistency with the findings of Beer and Sturm (1995) regarding beryllium saturation in the Zaifang sedimentary section and  $^{18}\delta$  in marine sediments. In both cases, there is a clear correlation between the fluctuations in beryllium saturation,  $^{18}\delta$ , and magnetic receptivity (fig 11).

When beryllium saturation and  $^{18}\delta$  decrease, there is a corresponding decrease in magnetic receptivity, indicating colder and drier climate conditions. Conversely, an increase in beryllium saturation and  $^{18}\delta$  is accompanied by an increase in magnetic receptivity, signifying warmer and more humid periods.

The high agreement between the climatic periods identified based on these parameters in the Zaifang sedimentary section and marine sediments, and the magnetic receptivity trends observed in the Nowdeh sedimentary section, highlights the synchrony of similar climate events in the past across different

locations. This consistency further supports the robustness of magnetic susceptibility as a proxy for understanding past climate variations and environmental changes (figure 11).

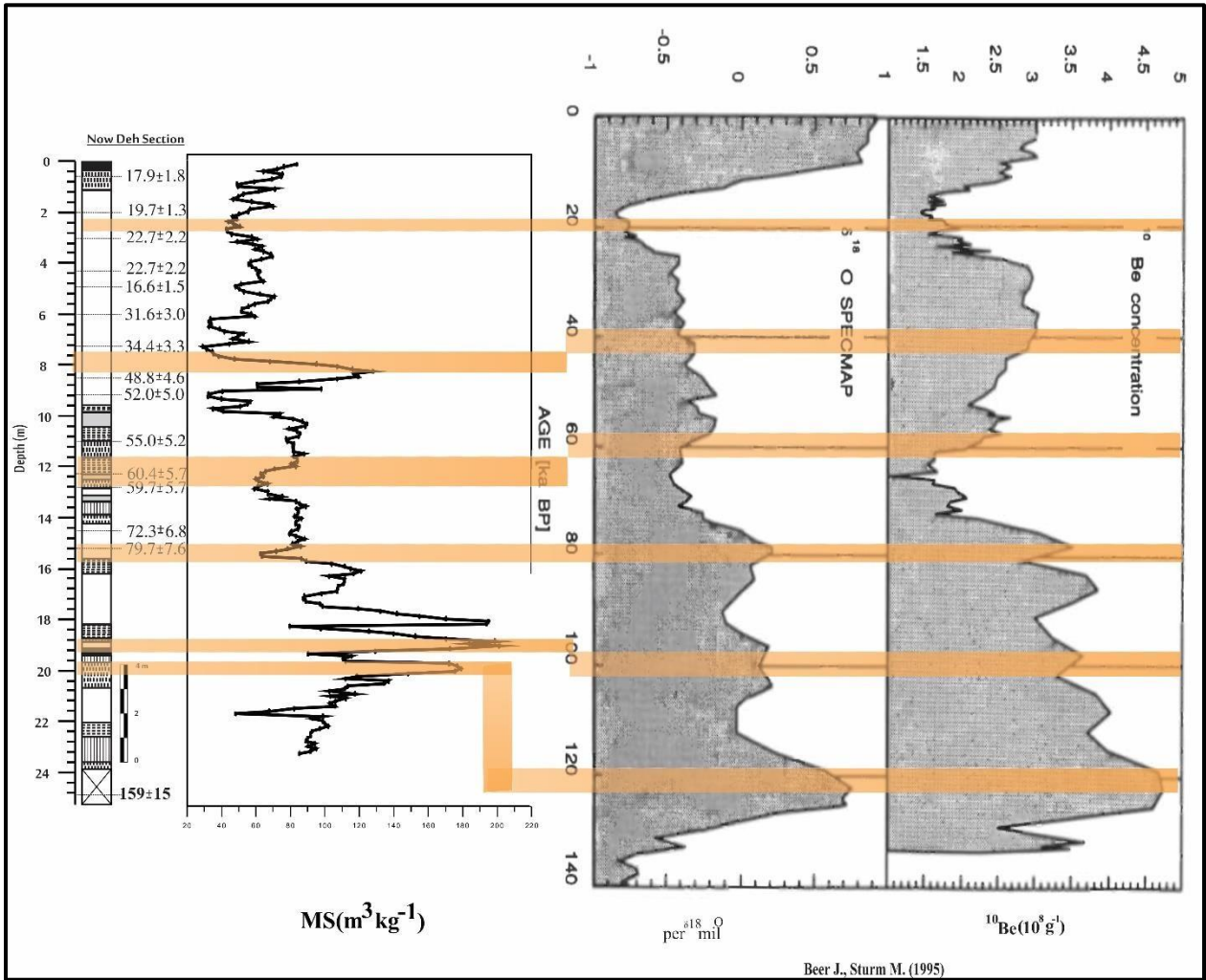


Figure 11: Comparison of magnetic receptivity results of Nowdeh sedimentary section in comparison with  $^{18}\text{O}$  and Be 10 isotope results of Xifeng sedimentary section (Beer and Sturm, 1995).

## Conclusion

In conclusion, the loess/paleosol sequences from Northeastern Iran serve as a valuable archive for studying the paleoenvironmental changes during the Upper Pleistocene. By employing a multi-proxy approach that integrates sedimentological, magnetic, and geochemical methods, the following key insights have been revealed:

1. The stratigraphy of the studied section aligns well with the typical pattern of Upper Pleistocene loess/paleosol successions in the region, providing valuable insights into the past environmental conditions.
2. Magnetic parameters show a strong correlation with climate conditions, making them effective variables for reconstructing climate change patterns in the region.
3. Comparisons between magnetic and geochemical data indicate that variations in geochemical weathering ratios mirror changes in magnetic weathering parameters, such as magnetic susceptibility, further enhancing our understanding of past environmental dynamics.
4. The high degree of coherence observed between the amplitudes of magnetic susceptibility and various geochemical ratios, including Rb/Sr, Mn/Ti, Zr/Ti, and Mn/Sr, reinforces the reliability of magnetic susceptibility as a proxy for tracking environmental changes and provides additional insights into the interplay between magnetic and geochemical processes.

Overall, this comprehensive multi-proxy analysis enhances our understanding of the paleoenvironmental changes in Northeastern Iran during the Upper Pleistocene period and emphasizes the importance of integrating sedimentological, magnetic, and geochemical data to unravel past climatic fluctuations and environmental dynamics.

## References

1. Ahmad, I., Chandra, R, 2013, Geochemistry of loess-paleosol sediments of Kashmir Valley, India: Provenance and weathering, *Journal of Asian Earth Sciences* 66, 73-89.
2. Antoine, P., Rousseau, D.D., Degeai, J.P., Moine, O., Lagroix, O., Kreutzer, S., Fuchs, M., Hatte, CH., Gauthier, C., Svoboda, J, and Lisa , I., 2013, High-resolution record of the environmental response to climatic variations during the Last Interglacial Glacial cycle in Central Europe: the loess-palaeosol sequence of Dolní Věstonice (Czech Republic), *Quaternary Science Reviews*, 67, PP 17-38.
3. Arias-Ortiz, A., et al. (2020). "The impact of climate change on soil chemistry and biogeochemical cycles." *Nature Reviews Earth & Environment*, 1(12), 689-702.
4. Bader N E, Broze E A, Coates M A, Elliott M M, McGann G E, Strozyk S, Burmester R F, 2024, The usefulness of the magnetic susceptibility of loess paleosol sequences for paleoclimate and stratigraphic studies: The case of the Quaternary Palouse loess, northwestern United States, *Quaternary International*, Article in Press.
5. Bai, Y., et al. (2022). "Rb/Sr ratio as a proxy for weathering and soil formation in the Loess Plateau, China." *Geoderma*, 410, 115754.

6. Baumgart, P., Hambach, U., Meszner, S., Faust, D., 2013. An environmental magnetic fingerprint of periglacial loess: records of Late Pleistocene loess paleosol sequences from Eastern Germany. *Quat. Int.* 296, 82–93.
7. Bloemendal J, Liu X, Sun Y, Li N, 2008, An assessment of magnetic and geochemical indicators of weathering and pedogenesis at two contrasting sites on the Chinese Loess plateau, *Palaeogeography, Palaeoclimatology, Palaeoecology* 257 (2008) 152–168.
8. Bloemendal, J., Xiuming L., Youbin, S., Ningning L., 2008. An assessment of magnetic and geochemical indicators of weathering and pedogenesis at two contrasting sites on the Chinese Loess plateau, *Palaeogeography, Palaeoclimatology, Palaeoecology* 257; 152–168.
9. Bronger, A., 2003. Correlation of loess-paleosol sequence in East and Central Asia with SE Central Europe: toward a continental Quaternary pedostratigraphy and paleoclimate history. *Quaternary International* 106/107, 11–31.
10. Buggle, B., Hambach, U., Glaser, B., Gerasimenko, N., Markovic, S., Glaser, I., Zöller, L., 2009. Stratigraphy, and spatial and temporal paleoclimatic trends in Southeastern/Eastern European loess–paleosol sequences. *Quat. Int.* 196, 186–206.
11. Chen, J., An, Z.S., Head, J., 1999. Variation of Rb/Sr ratios in the loess–paleosol sequences of central China during the last 130,000 years and their implications for monsoon paleoclimatology. *Quaternary Research* 51, 215–219.
12. Chen, T., Xie, Q., Xu, H., Chen, J., Ji, J., Lu, J., Lu, H and Balsam, W, 2010, Characteristics and formation mechanism of pedogenic hematite in Quaternary Chinese loess and paleosols, *Catena* 81, 217–225.
13. Chen, Y., Wang, X., & Li, J. (2022). Impact of climate fluctuations on vegetation patterns in arid regions: Case study from northwestern China. *Quaternary Science Reviews*, 265, 106552.
14. Chlachula, J., Little, E., 2011, A high-resolution Late Quaternary climatostratigraphic record from Iskitim, Priobie Loess Plateau, SW Siberia, *Quaternary International* 240, 139e149
15. Ding, Z.L., Ranov, V., Yang, S.L., Finaev, A., Han, J.M., Wang, G.A., 2002. The loess record in southern Tajikistan and correlation with Chinese loess. *Earth and Planetary Science Letters* 200, 387e400.
16. Ding, Z.L., Yang, S.L., Sun, J.M., Liu, T.S., 2001. Iron geochemistry of loess and Red Clay deposits in the Chinese Loess Plateau and implications for long-term Asian monsoon evolution in the last 7.0 Ma. *Earth and Planetary Science Letters* 185, 99–109.
17. Fischer, P., Hilgers, A., Protze, J., Kels, H., Lehmkuhl, F., Gerlach, R., 2012. Formation and geochronology of Last Interglacial to Lower Weichselian loess/palaeosol sequences — case studies from the Lower Rhine Embayment, Germany. *E & G Quat.Sci. J.* 61, 48–63.
18. Fitzsimmons, K.E., Marković, S.B., Hambach, U., 2012. Pleistocene environmental dynamics recorded in the loess of the middle and lower Danube Basin. *Quat. Sci. Rev.* 41,104–118.
19. Forster, T., Evans, M.E., Havlíček, P., Heller, F., 1996. Loess in the Czech Republic:magnetic properties and paleoclimate. *Stud. Geophys. Geod.* 40, 243–261.
20. Frechen, M., Kehl, M., Rolf, C., Sarvati, R., Skowronek A., 2009, Loess Chronology of the Caspian Lowland in Northern Iran, *Quaternary International*, No. 198, pp. 220–233.

21. Frechen, M., Oches, E.A., Kohfeld, K.E., 2003. Loess in Europe—mass accumulation rates during the Last Glacial Period. *Quaternary Science Reviews* 22, 1835–1875.
22. Gallet, S., Jahn, B.M., Torii, M., 1996. Geochemical characterization of the Luochuan loess-paleosol sequence, China, and paleoclimatic implications. *Chemical Geology* 133, 67–88.
23. Gocke, M., Hambach, U., Eckmeier, E., Schwark, L., Zöller, L., Fuchs, M., Löscher, M., Wiesenberg, G.L.B., 2014. Introducing an improved multi-proxy approach for paleoenvironmental reconstruction of loess–paleosol archives applied on the Late Pleistocene Nussloch sequence (SW Germany). *Palaeogeogr. Palaeoclimatol. Palaeoecol.* 410, 300–315.
24. Guanhua. L, Dunsheng. X, Ming. J, Jia. J, Jiabo. L, Shuang Z, Yanglei. W, 2014, Magnetic characteristics of loess/paleosol sequences in Tacheng, northwestern China, and their paleoenvironmental implications, *Quaternary International*, 3, 1-10.
25. Guo, Z.T., Ruddiman, W.F., Hao, Q.Z., Wu, H.B., Qiao, Y.S., Zhu, R.X., Peng, S.Z., Wei, J.J., Yuan, B.Y., and Liu, T.S., 2002. Onset of Asian desertification by 22 Myr ago inferred from loess deposit in China. *Nature* Vol. 416, pp. 159–163.
26. Harrison, S. P., Prentice, I. C., & Baird, A. J. (2020). Vegetation and climate change: Implications for ecosystem services. *Global Change Biology*, 26(2), 429-445.
27. Heller, F., Liu, T., 1984. Magnetism of Chinese loess deposits. *Geophys. J. R. Astron. Soc.* 77, 125–141.
28. Hosek J., Hambach U., Lisa L., Grygar T.M., Horacek I., Meszner S., Knesl I., 2015, An integrated rock-magnetic and geochemical approach to loess/paleosol sequences from Bohemia and Moravia (Czech Republic): Implications for the Upper Pleistocene paleoenvironment in central Europe, *Palaeogeography, Palaeoclimatology, Palaeoecology*, 418, pp. 344-358.
29. Hošek, J. Hambach, U. Lisá, L. Matys G. T. Horáček, I., 2015, an integrated rock-magnetic and geochemical approach to loess/paleosol sequences from Bohemia and Moravia (Czech Republic): Implications for the Upper Pleistocene paleoenvironment in central Europe, *Palaeogeography, Palaeoclimatology, Palaeoecology* 418, 344–358.
30. Huang, G., Liu, J., Zhang, L., & Zhang, X. (2022). Magnetic susceptibility of loess deposits as a proxy for paleoenvironmental changes: Implications for climate variations in North China. *Journal of Quaternary Science*, 37(5), 639-652.
31. Jary, Z., Ciszek, D., 2013. Late Pleistocene loess–palaeosol sequences in Poland and western Ukraine. *Quat. Int.* 296, 37–50.
32. Jiang, Y., et al. (2020). "Soil organic carbon dynamics in response to climate change: A review." *Global Change Biology*, 26(5), 1-16.
33. Jordanova D, Jordanova N, 2024, Geochemical and mineral magnetic footprints of provenance, weathering and pedogenesis of loess and paleosols from North Bulgaria, *Catena*, Volume 243, 108131.
34. Jordanova, D., Grygar, T., Jordanova, N., Petrov, P., 2011. Palaeoclimatic significance of hematite/goethite ratio in Bulgarian loess–palaeosol sediments deduced by DRS and rock magnetic measurements. In: Petrovsky, E., Ivers, D., Harinarayana, T., Herrero- Bervera, E. (Eds.), the Earth's Magnetic Interior. IAGA Special Sopron Book Series. Springer Verlag, Berlin.

35. Karimi, A., Khademi, H., Ayoubi, A., 2013, Magnetic susceptibility and morphological characteristics of a loess–paleosol sequence in northeastern Iran, *Catena*, 101, pp. 56-60.
36. Karimi, A., Khademi, H., Jalalian, A., 2011, Loess: Characterize and application for paleoclimate study, *Geography Research*, Volume 76, pp1-20.
37. Karimi, A., Khademi, H., Kehl, M., Jalaian, A., 2009, Distribution, Lithology and Provenance of Peridesert Loess Deposits in Northeast Iran, *Geoderma*, No.148, pp. 241-250.
38. Kehl, M., Frechen, M., Skowronek, A., 2005, Paleosols Derived from Loess and Loesslike Sediments in the Basin of Persepolis, Southern Iran, *Quaternary International*, No.140/141, pp.135-149.
39. Kehl, M., Sarvati, R., Ahmadi, H., Frechen, M., Skowronek, A., 2006, Loess / Paleosol sequences along a Climatic Gradient in Northern Iran, *Eiszeitalter und Gegenwart*, No. 55, pp.149-173.
40. Lateef, A.S.A., 1988. Distribution, provenance, age and paleoclimatic record of the loess in Central North Iran. In: Eden, D.N., Furrer, R.J. (Eds.), *Loess – its Distribution, Geology and Soil*. Proceeding of an International Symposium on Loess, New Zealand, 14–21 February 1987. Balkema, Rotterdam, pp. 93–101.
41. Makeev A, Rusakov A, Kust P, Lebedeva M, Khokhlova O, 2024, Loess-paleosol sequence and environmental trends during the MIS5 at the southern margin of the Middle Russian Upland, *Quaternary Science Reviews* Volume 328, 108372.
42. Mehdipour, F, 2012, Investigation of paleoclimate in late quaternary western alborz using of technical applied and magnetism parameters, *Geology and Mineral Exploration*, master science thesis.
43. Nabavi, Mehdi, 1976, *Introduction geology of Iran*, pp1-109.
44. Okhravi, R. Amini, A., 2001, Characteristics and Provenance of the Loess Deposits of the Gharatikan Watershed in Northeast Iran, *Global and Planetary Change*, No. 28, pp.11-22.
45. Pashaei, A., 1996, Study of Chemical and Physical and Origin of Loess Deposits in Gorgan and Dasht Area, *Earth Science*, 23/24, pp. 67-78.
46. Prins, M.A., Vriend, M., Nugteren, G., Vandenbergh, J., Huazuo, L., Zheng, H., Weltje, G.J., 2007. Late Quaternary aeolian dust input variability on the Chinese Loess Plateau: inference from unmixing of loess grain-size record. *Quaternary Science Reviews* 26, 230– 242.
47. Schatz, A.-K., Scholten, T., Kühn, P., 2014. Paleoclimate and weathering of the Tokaj (NE Hungary) loess–paleosol sequence: a comparison of geochemical weathering indices and paleoclimate parameters. *Clim. Past Discuss.* 10, 469–507.
48. Song, Y., Shi, Z., Dong, H., Nie, J., Qian, L., Chang, H. & Qiang, X., 2008- Loess Magnetic Susceptibility in Central Asia and its Paleoclimatic Significance. *IEEE International Geoscience & Remote Sensing Symposium*, II 1227-1230, Massachusetts.
49. Spassov, S., 2002. Loess Magnetism, Environment and Climate Change on the Chinese Loess Plateau. Doctoral Thesis, ETH Zürich, pp. 1–151.
50. Taylor, S.R., McLennan, S.M., McCulloch, M.T., 1983. Geochemistry of loess, continental crustal composition and crustal model ages. *Geochimica et Cosmochimica Acta* 47, 1897– 1905.

- 750 51. Tzedakis, P. C. (1994), Hierarchical biostratigraphical classification of long pollen sequences,  
751 Journal of quaternary science, volume 9, issue 3, pp 257-259.
- 752 52. Zhang, Q., Chang, I., & Luo, Z. (2021). Response of vegetation to climate change over the past  
753 millennium in Eurasia. *Climate Dynamics*, 56(1), 75-88.
- 754 53. Zhang, X., et al. (2021). "Using Rb/Sr ratios to assess weathering intensity in loess profiles."  
755 *Earth Surface Processes and Landforms*, 46(12), 2454-2466.
- 756 54. Zhu, K., et al. (2021). "Leaching of soil nutrients under different climate scenarios." *Journal of*  
757 *Geophysical Research: Biogeosciences*, 126(7).